A microscopy approach for *in situ* inspection of the μCMM stylus for contamination

A microscopy approach for *in situ* inspection of the µCMM stylus for contamination

Xiaobing Feng[1], Jonathan Pascal[2], Simon Lawes[1]

[1]The University of Nottingham, UK

[2]École nationale d'ingénieurs de Saint-Etienne, France

Abstract

During the µCMM measurement process, contamination gradually builds up on the surface of the stylus tip and affects dimensional accuracy of the measurement. Regular inspection of the stylus for contamination is essential in determining the appropriate cleaning interval and preventing the dimensional error from becoming significant. However, *in situ* inspection of a µCMM stylus is challenging due to the size, spherical shape, material and surface properties of a typical stylus. To address the challenges, this study evaluates several non-contact measurement technologies for *in situ* stylus inspection and based on those findings proposes a cost-effective microscopy approach. The operational principle is then demonstrated by an automated prototype, coordinated directly by the CMM software MCOSMOS, with an effective threshold of detection as low as 400 nm and large field of view and depth-of-field. The level of stylus contamination on the stylus has been found to increase steadily with the number of measurement contacts made. Once excessive contamination is detected on the stylus, measurement should be stopped and stylus cleaning procedure should be performed to avoid affecting measurement accuracy.

Keywords: µCMM, stylus inspection, contamination, microscopy, focus stacking.

1. Introduction

Measurement of geometry of precision parts is often conducted on a micro-coordinate measurement machine (µCMM), in part due to the straightforward interpretation of measurement data relative to optical measurement systems. Typically, features with millimetre to micrometre size are expected to be measured with sub micrometre accuracy. However, during measurement, contact between the stylus and the sample is likely to cause debris to attach to the stylus tip [1-4], introducing error to that measurement and future measurements as shown in Figure 1. The stylus tip used in a µCMM is often 300 µm or less in diameter to allow access to small features. As the size of stylus decreases, the effect of contamination induced error has become more significant than with traditional CMMs. The smallest stylus commercially available is equipped with a 125 µm ruby sphere for use on Zeiss F25 µCMM, while research efforts have produced stylus tips with sub 100 µm diameter out of a single piece of metal with electro-discharge machining (EDM) and electrochemical machining (ECM) processes [5-7]. In those cases, debris a few micrometres in size may cause dimensional errors that are orders larger than what is typically reported [2, 8]. Therefore it is essential to keep the stylus clean for precision measurement.

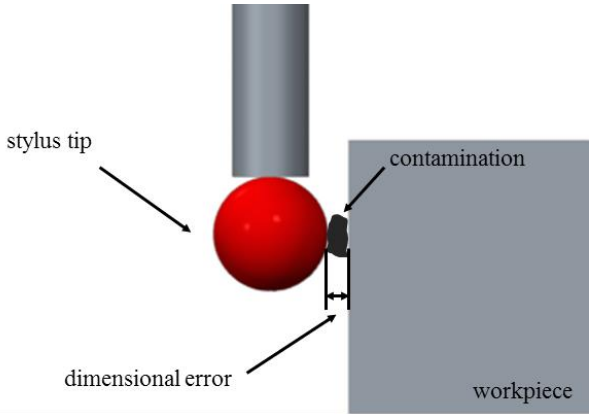

Figure 1. Illustration of debris-induced measurement error.

ISO standard 10360-5 requires that cleaning procedure of the stylus tip be conducted before measurement tests [9], but lacks reference to any inspection procedure to verify cleanliness of the stylus tip. Previous studies [1, 10] have investigated the effectiveness of various cleaning technologies in removing contamination from µCMM stylus tips and have identified CO_2 snow cleaning as an effective and safe technology to achieve this. Subsequently, a prototype snow cleaning device has been developed [11] by the authors for *in situ* cleaning of µCMM stylus tips. Essential to the cleaning procedure is a method of inspecting the stylus for contamination to determine appropriate cleaning interval and to qualify the stylus in terms of cleanliness. Common practice of stylus inspection is conducted offline. The operator removes the stylus from the CMM system and examines with another instrument such as an optical microscope or scanning electron microscope. Such inspection procedure disrupts the measurement process, risks introducing error due to human handling and is time consuming. This study presents a novel approach for *in situ* inspection of the µCMM stylus. The development of the approach begins with a review of existing microscopy and surface measurement technologies against the following technical and practical considerations.

Requirements:

- Small proportion of the cost of a µCMM.
- Ability to resolve debris down to sub-micrometer scale.
- Ability to differentiate organic & metallic debris.
- Ability to integrate with the µCMM.

Desirables:

- Short measurement interval, less than 60 seconds.
- Minimal handling of the stylus.
- Sufficient field of view to cover the horizon of the stylus tip.
- Ability to provide volume/height measurement of debris.

The rest of this article is structured as follows. In section 2, existing technologies including scanning electron microscopy, reflected light microscopy, confocal microscopy, coherence scanning interferometry, focus variation microscopy and laser point autofocus profilometry are evaluated using a stylus with a ruby tip. Based on the evaluation, a microscopy approach coupled with focus stacking technique for stylus inspection is proposed and demonstrated in section 3. Section 4 describes and further demonstrates an *in situ* stylus inspection device developed using the proposed approach with a low end microscope. The device communicates with the CMM software to automate the inspection procedure. Progressive build-up of contamination on the stylus during measurement was successfully observed using the developed device. Finally, section 5 concludes the findings and contribution of this study.

2. Evaluation of inspection technologies

Six types of inspection technologies have been selected for evaluation to be the foundation of the contamination inspection approach. Table 1 describes the instrument being evaluated for each technology and the conditions used. Two levels of magnification were used for image-based technologies:

- a high magnification level to obtain the best details of the stylus tip surface and;
- a low magnification level with the entire stylus tip in the field of view (FoV).

The ideal operation would be to capture the entire stylus tip in the FoV, but many of the technologies support the stitching of larger areas. Imaging at a high and a low magnifications allows both operating conditions to be considered. Lateral resolution for each evaluated technology is determined using the larger value between the pixel spacing and the optical resolution calculated using the Rayleigh criterion.

Scanning electron microscopy (SEM) was chosen as a reference because it has been shown to produce high resolution and contrast images of surface contamination on stylus tips in previous studies [1, 11]. Due to the different operating principles involved, magnification of the SEM is not comparable with microscopy technologies. Also point autofocus profilometry measures by sensing the position of the laser spot instead of analysing the obtained image; therefore magnification has no significant influence on resolution.

Table 1. List of evaluated technologies and maginification.

Technology	Instrument	Low magnification	High magnification
scanning electron microscopy	Hitachi S-2600N	250×	2500×
reflected light microscopy	Nikon LV100ND	20×	100×
confocal microscopy	Sensofar S Neox	N/A	50×
coherence scanning interferometry	Bruker ContourGT	20×	50×
focus variation microscopy	Alicona InfiniteFocus	50×	100×
laser point autofocus profilometry	Mitaka MLP-3SP	N/A	N/A

A μCMM stylus (Renishaw A-5000-7800) with a 300 μm diameter tip was used to evaluate all the inspection technologies. The stylus tip is made of ruby, the most common choice of material for its wear-resistance and low cost. Contamination was introduced to the stylus tip through repeated probing on a milled brass surface (Sq = 2.81 μm, λc = 0.8 mm) at various orientations. The brass sample was manufactured in the Precision Manufacturing Centre at the University of Nottingham and has been cleaned in an ultrasonic bath after being machined. The preparation procedure ensured debris of different material and form are scattered around the usable surface of the stylus tip.

2.1 Scanning electron microscopy

SEM produces images of a sample by detecting the interaction between a beam of electrons and the sample surface. The focused electron beam is pointed at one point at a time and raster scanned through a surface to form an image. As magnification increases, SEM is commonly able to capture details in the nanometre scale.

Figure 2 shows SEM micrographs of the prepared μCMM stylus tip obtained using back-scattered electron (BSE) imaging. The two images were obtained with accelerating voltage of 25 kV and 30 kV respectively, and working distance of 9.5 mm.

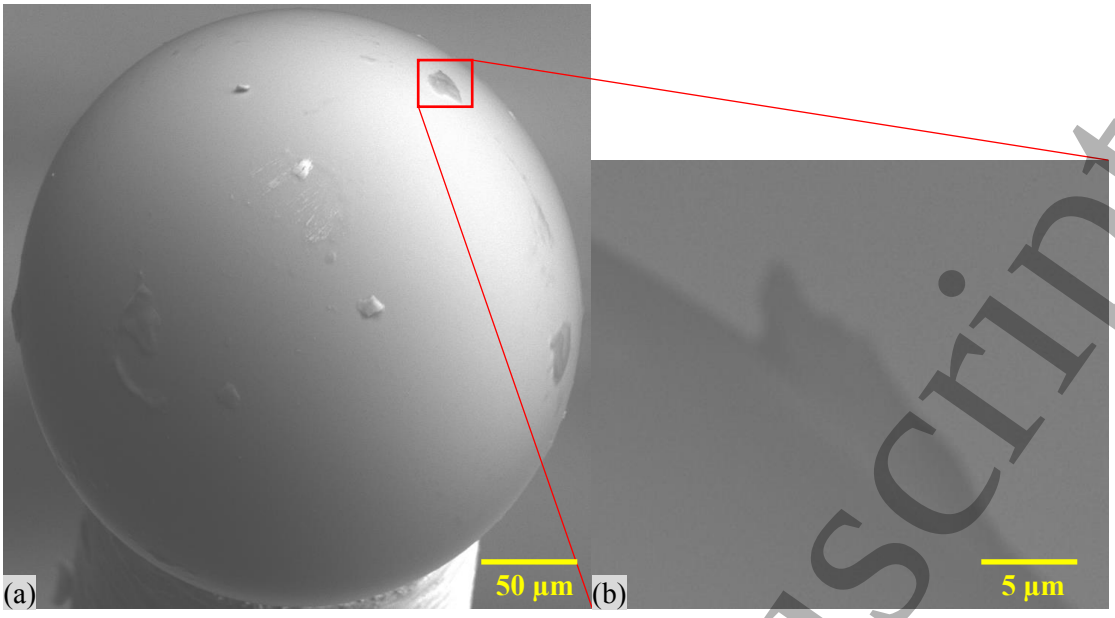

Figure 2. BSE SEM micrographs of a 300 µm ruby tip (a) at 250× magnification and (b) at 2500× magnification.

On the top of the sphere, metallic debris can be seen to have a bright appearance. In contrast, organic debris appears darker due to their lower atomic number. With the sphere in the FoV, the SEM micrograph has a good depth-of-field (DoF) and is not affected by the smooth surface or the high slope angle of the sphere. Resolution at this magnification is approximately 0.4 µm, limited by pixel spacing.

2.2 Reflected light microscopy

The second technology evaluated was reflected light microscopy (RLM), also known as bright field microscopy, here using epi-illumination.

Figure 3 shows microscope images of the prepared µCMM stylus tip with epi-illumination. Metallic particles are clearly observed with better contrast than in grey scale SEM micrographs. With the sphere in the FoV, the optical resolution is approximately 0.7 µm by Rayleigh criterion as the numerical aperture (NA) of the objective is 0.45; and sub-micrometre debris can be resolved. At 100× magnification, the optical resolution is further improved to approximately 0.3 µm (NA = 0.9).

It is clear that both images are significantly limited in DoF. At 20× magnification, the image has a DoF of approximately 6 µm, which is 1/25 of the full depth required to image the entire hemisphere. At 100× magnification, DoF is less than 1 µm.

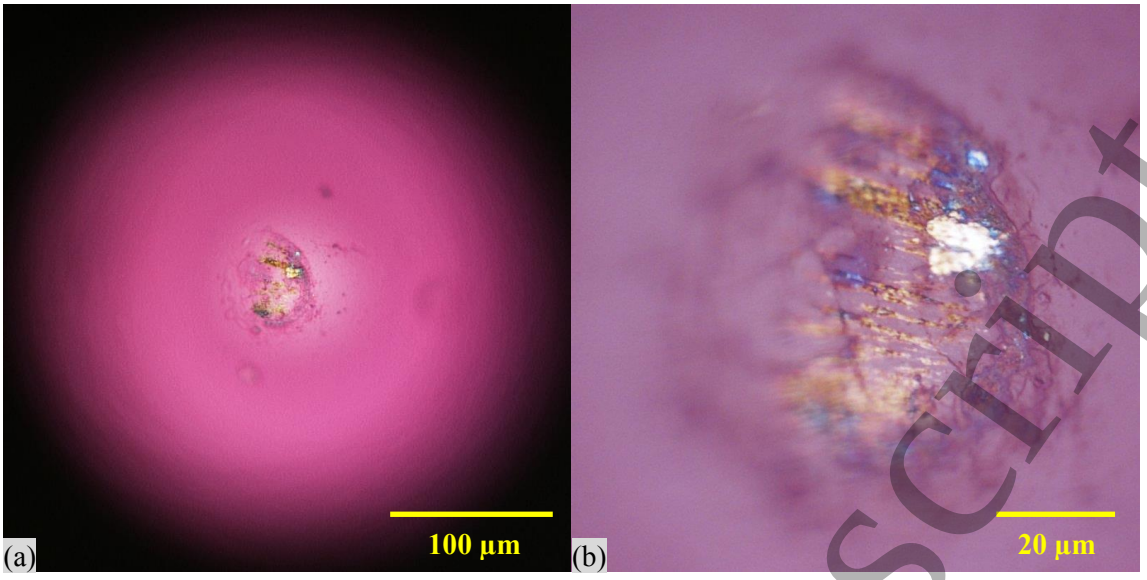

Figure 3. Microscope images of metallic contamination on the surface of a 300 µm ruby tip (a) at 20× magnification and (b) at 100× magnification.

Figure 4 shows that contamination at different surface heights, even around the azimuth of the sphere, can be clearly imaged. This demonstrates that high slope angle does not affect imaging.

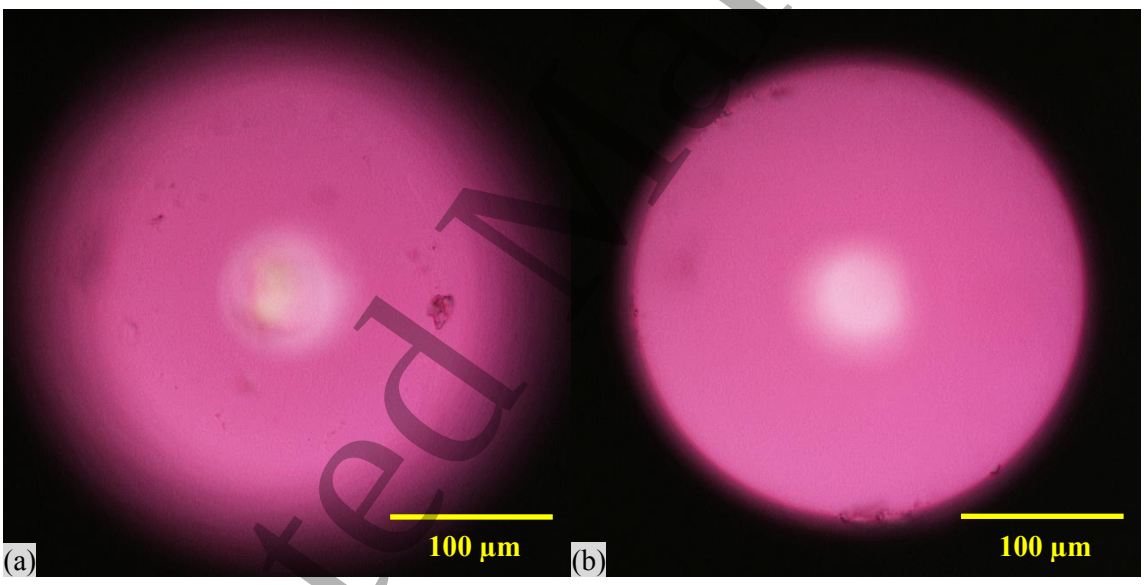

Figure 4. Microscope images of a 300 µm ruby tip at 20× magnification focused (a) on approximately 45º slope angle and (b) around azimuth.

2.3 Confocal microscopy

Confocal microscopy (CM) places a pinhole at the confocal plane in front of the detector. Any out-of-focus light is effectively eliminated and only details at a certain depth are imaged. Reconstruction of the 3D surface is achieved by raster scanning or by illuminating the surface with structured patterns. Resolution of the technology is superior to optical microscopy as a shorter wavelength illumination source is often used in combination with objectives with high NA.

Figure 5 shows the topography of the prepared µCMM stylus tip obtained using a micro-display type confocal microscope.

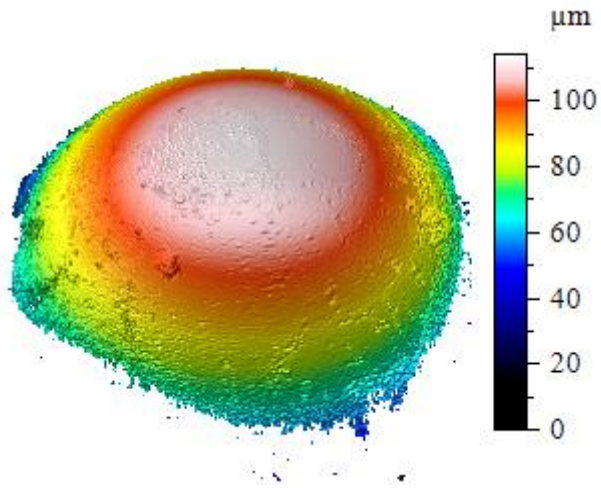

Figure 5. Surface topography of a 300 µm ruby tip obtained by CM at 50× magnification.

Unlike SEM and optical microscopy, confocal microscopy does not provide colour or material information of the sample. However it has the advantage of providing topographic 3D surface measurements that can be used to determine the volume of contamination by removal of spherical form. At 50× magnification (NA = 0.95), lateral resolution is about 0.3 µm. Reasonably good measurement is achieved up to a slope angle of 50 °, beyond which signal-to-noise ratio deteriorates rapidly as shown in Figure 5.

2.4 Coherence scanning interferometry

Coherence scanning interferometry (CSI) is also known as white light interferometry. A coherent light source is split into two beams: one reflects on the sample surface and the other reflects on a reference mirror. By recombining the two beam paths on a detector, an interference pattern is formed. By analysing the interference patterns while scanning along the surface height direction, topography of the sample surface is measured. Lateral resolution is similar to optical microscopy as the technology relies on analysis of the images obtained.

Figure 6 shows the topography of a µCMM stylus tip measured by CSI using white light illumination.

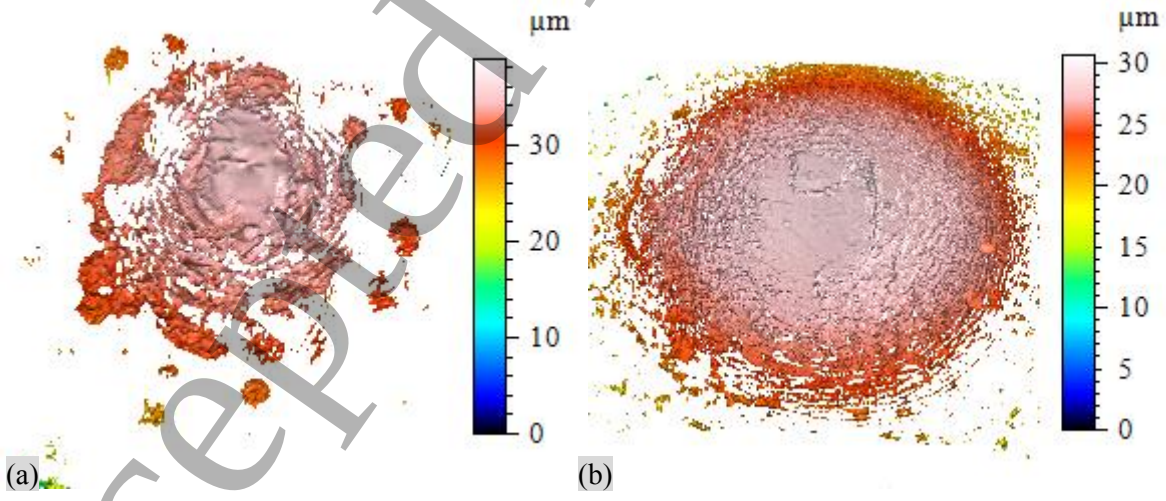

Figure 6. Surface topography of a 300 µm ruby tip obtained using CSI (a) at 20× magnification and (b) at 50× magnification.

The CSI technology also provides topographic information that may be important in determining volume of contamination; however colour information is completely lost. At 20× magnification the entire sphere is in the FoV, however the surface is only measured to a slope angle less than 5 °. Optical resolution is approximately 0.8 µm (NA = 0.4). At 50× magnification, FoV is reduced to

126 µm × 95 µm and optical resolution is approximately 0.6 µm (NA = 0.55). The surface is able to be measured up to a slope angle of 10 °. Due to lower NA of the objectives used, lateral resolution and slope tolerance are typically inferior to CM at the same magnification.

2.5 Focus variation microscopy

Focus variation microscopy (FVM) technologies computes topographic data from a stack of images of the sample surface captured at numerous heights at the sample surface. The image stack is then analysed to determine the surface height at each pixel location by searching for maximum pixel contrast through the stack. As the technology relies on the change in contrast, surface roughness is required in order for the instrument to function properly. Lateral resolution of FVM is determined by the image and optical resolution as well as the contrast searching algorithm, and cannot be easily determined. Therefore, the estimated lateral resolution specified by the instrument software and recorded along with the measurement data is given here.

Figure 7 shows the topography of a µCMM stylus tip obtained with FVM at 50× magnification using coaxial light illumination.

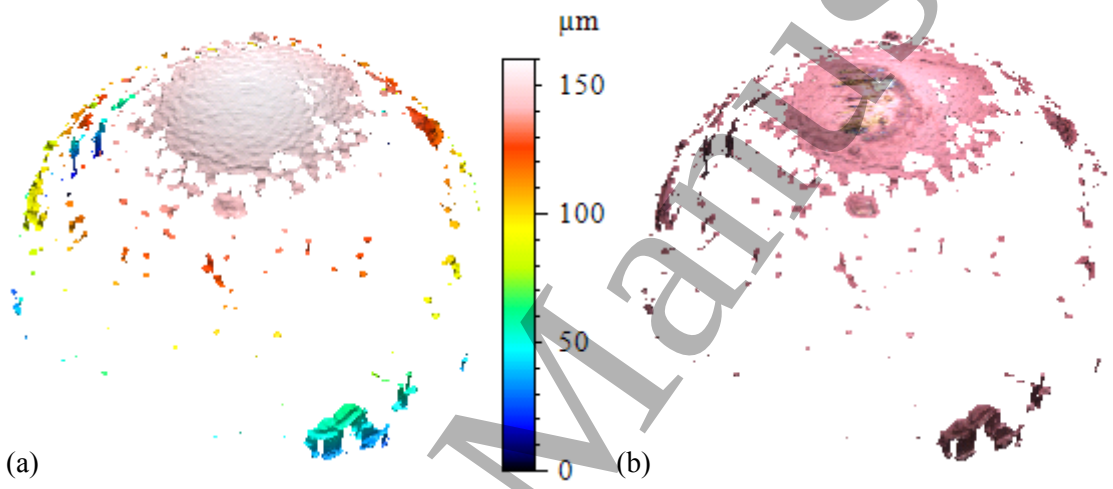

Figure 7. Surface of a 300 µm ruby tip obtained by FVM at 50× magnification, presented in the form of (a) topography and (b) colour image.

By overlaying the focused microscope image of individual areas onto the topography, additional colour information is preserved. This is helpful in correlating the size and material of the contamination. Topography of the ruby surface is captured quite well to a slope angle of 20 °, with less than 5% non-measurement area, which is considered adequate for imaging contamination. In addition, debris located in many areas close to the azimuth plane has been systematically detected. Since contamination is the matter of interest, FVM is considered to measure up to a slope angle of 90 °, though the relative certainty with which contamination can be detected is not clear.

Lateral resolution specified by the software for this measurement is approximately 1 µm. However, measurement artefacts in the form of waviness and steps have been observed throughout the surface. As a result, accuracy of contaminant volume is significantly affected.

To evaluate the best performance of measuring contamination volume, another measurement was conducted at 100× magnification as shown in Figure 8, where an area of 162 µm × 162 µm on the top of the sphere was measured.

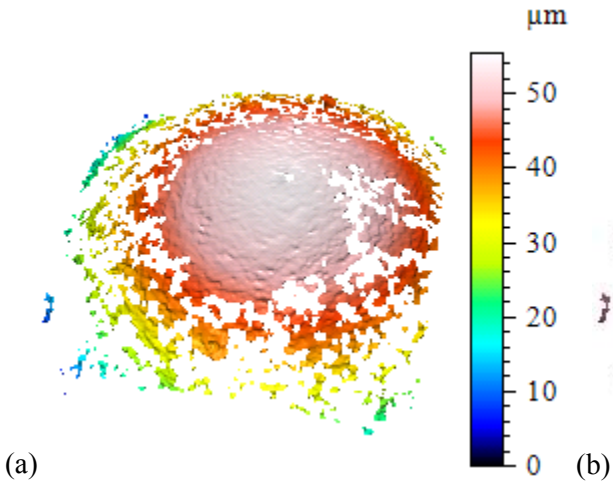

Figure 8. Surface of a 300 µm ruby tip obtained by FVM at 100× magnification, presented in the form of (a) topography and (b) colour image.

At 100× magnification, lateral resolution estimated by the instrument software is 0.8 µm. Debris is observed with better details than at 50× magnification. However, measurement artefacts in topography are still too significant to be separated from contamination. The ruby surface is able to be measured up to a slightly higher slope of 25 °.

For this instrument there is the option of using polarising filters, however those were not found to provide noticeable improvement.

2.6 Point autofocus profilometry

Point autofocus profilometry (PAP) measures the surface by automatically focusing a laser beam onto a point on the sample surface. Automatic focusing is achieved by moving the microscope height relative to a point on the surface, in order to maintain a predefined working distance. Through the accurate movement of the sample stage in *X*- and *Y*-directions as well as movement of the microscope in *Z*-direction, the 3D surface texture can be measured. Advantage of PAP is that lateral resolution of measurement is determined by the positioning accuracy of the stage and the microscope, and can be as low as 0.1 µm independent of magnification. Disadvantage is that 3D surface measurement is very slow compared to other optical technologies.

Figure 9 shows the topography of a µCMM stylus tip obtained by PAP using index mode for accurate measurement, with 1 µm pitch distance. Due to low measurement speed, only an area of 100 µm × 100 µm on the top of the sphere has been measured.

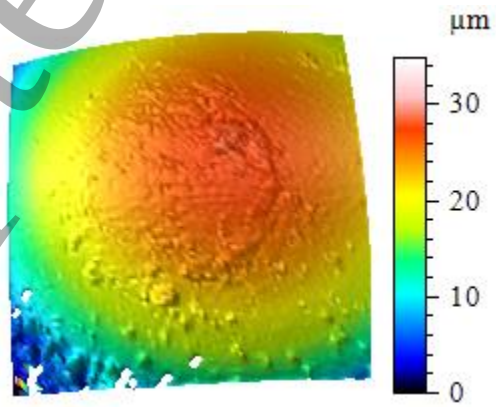

Figure 9. Surface topography of a 300 µm ruby tip obtained by PAP with 1 µm pitch distance.

Similar to CM and CSI, PAP provides surface topography but loses colour information. The ruby surface measured up to a slope angle of 40 °, beyond which the signal-to-noise ratio drops until at 45 °

the returned light is no longer sufficient to determine surface height. Although the highest lateral resolution is 0.1 μm, such setting is not attempted due to long measurement period required.

2.7 Discussion

The main characteristics of the six evaluated inspection technologies relevant to the inspection of μCMM styli for surface contamination are summarised in Table 2, which are used to decide whether the technologies are suitable candidates for the *in situ* stylus inspection prototype. The evaluation has identified several challenges for inspection technologies.

In the absence of topography, 2D image of the sphere with sufficient resolution is the best choice to determine the amount of contamination on the stylus. SEM is able to provide sub-micrometre resolution with the entire sphere in the FoV and can inspect the sphere up to 90 ° of slope angle. However, SEM inspection takes much more than a few minutes and cannot inspect the stylus *in situ*, as it requires a sealed vacuum chamber for imaging. Therefore, SEM micrographs are more useful as a reference for comparing with other measurement results.

RLM is also capable of sub-micrometre resolution with the entire sphere in the FoV and can inspect the sphere up to 90 ° of slope angle. However, the disadvantage of RLM is the limited DoF, which will require vertical scanning to capture the entire hemisphere.

Spherical geometry of the stylus tip presents challenges due to both the presence of high surface slope angles and the need for a large depth of field or vertical scanning. *In situ* stylus inspection requires that the entire front hemisphere of the tip be inspected in a single procedure of less than a few minutes. Since none of the commercial μCMM systems are able to rotate the stylus, technologies that are sensitive to surface slope angle cannot measure the entire hemisphere as required. In theory, instruments can be modified to move around the stylus and measure at various angles to cover the entire sphere, but multiple measurements may be time consuming and not all angles are accessible due to instrument size. Among the evaluated technologies, only SEM, RLM and FVM are able to inspect the sphere up to 90 ° slope angle. However, FVM does not have sufficient resolution at such magnification, with the effective resolution being lower than the optical resolution of the images due to the topography reconstruction process.

Optical properties of ruby (Al_2O_3) tips, commonly used for μCMM styli, further limit the performance of optical systems. Transparency of the material makes features (e.g. voids, cracks, internal structures) underneath the sphere surface visible. The specular surface further affects measurement performance, especially at high slope angles due to low return of diffusely reflected light.

Topography measurement is the best approach for determining the amount of contamination on the stylus, but every topography measurement obtained in the study except CM shows the presence of measurement artefacts and therefore cannot be used to determine the volume of contamination without careful consideration. Correction methods to remove the artefacts from the results will require in-depth investigation into the instruments' transfer function, which is not readily available for CMM users.

Table 2 Evaluation of non-contact inspection technologies

Technology	Instrument	Highest lateral resolution	Lateral resolution with sphere in FoV	Measure smooth surface	Maximum slope angle	Measure contamination volume in 3D	Cost of typical instrument
SEM	Hitachi S-2600N	5 nm	0.4 µm	Yes	90 º	No	> £100k
RLM	Nikon LV100ND	0.3 µm	0.7 µm	Yes	90 º	No	< £10k
CM	Sensofar S Neox	0.3 µm	N/A	Yes	50 º	Yes	£50k - £150k
CSI	Bruker ContourGT	0.6 µm	0.8 µm	Yes	10 º	Yes	£70k - £200k
FVM	Alicona InfiniteFocus	0.8 µm	1 µm	No	90 º	Yes	£20k - £150k
PAP	Mitaka MLP-3SP	0.1 µm	N/A	Yes	40 º	Yes	> £200k

Based on the above analysis, among the evaluated technologies, RLM is determined to be a suitable candidate for further development, and a microscopy approach for stylus inspection is proposed by incorporating RLM with focus stacking technique. The limited DoF of RLM can be overcome by taking multiple images at different height levels and reconstructing a full depth-of-field (FDoF) image where the entire hemisphere appears in focus without sacrificing resolution. Such technology is known as focus stacking and is commonly used by photographers shooting in macro lens. Focus stacking is fast, low cost, amenable to miniaturisation and gives adequate observation of contamination, though it lacks volumetric measurement.

3. Reflected light microscopy for stylus inspection

Based on the findings of the experimental review, it is clear that epi-illuminated RLM offers an effective, low cost means of detecting the presence of debris on µCMM styli. However, there remains a number of practical challenges (e.g. narrow DoF, reflection of illumination source) in implementing such a system. In the following sections, this paper will illustrate the solution to some of these challenges.

A microscope is used to capture a stack of images across the required range of focal depth. An image processing algorithm then searches through the stack of images and for each pixel finds the layer that shows the highest contrast to its neighbours. These pixels are determined to have been at the focal plane of the image. The focused pixels are then composited into a single image for inspection. Various versions of proprietary and free software are readily available, where the main difference lies in the contrast searching method and user interface. This study has chosen Zerene Stacker for reconstruction of the FDoF image, from which better results have been obtained for this particular application. The same microscope evaluated in the last section has been used to capture the stack of images.

To demonstrate the capability of the proposed microscopy approach, two µCMM styli with ruby tips and diameters of 300 µm (Renishaw A-5000-7800) and 125 µm (Zeiss 620151-8401-000) respectively have been inspected using the following steps:

- Choose an appropriate magnification to image the tip in the FoV. Adjust sample height to focus onto the nearest face of the sphere, as shown in Figure 10.
- Capture an image with the microscope.
- By moving the microscope stage, manually move the stylus up towards the lens by a distance Δz, which should be similar to the DoF of the objective. Then capture an image with the microscope.
- Repeat the last step until the focal plane coincides with azimuth plane of the sphere. Then capture the last microscope image.

After the stack of images has been captured, Zerene Stacker is used to reconstruct the FDoF image using 'PMax' mode, an implementation of the pyramid method for image data processing [12, 13].

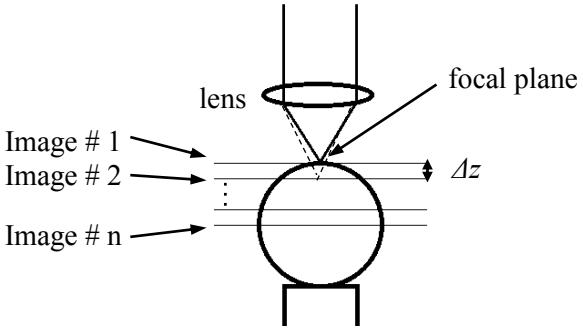

Figure 10. Illustration of image stack capturing procedure.

3.1 Stylus #1: 300 µm diameter

The first stylus being inspected is the same prepared stylus previously used for evaluating the imaging technologies. The stylus was imaged at 20× magnification with epi-illumination. DoF of the objective (plan-fluorite, NA = 0.45) is approximately 6 µm. Therefore, a series of 25 images were captured with step distance Δz = 6 µm in order to cover the entire hemisphere. Figure 11 shows the images of the sphere focusing, from left to right, at the top of the sphere, at two intermediate height levels and at the azimuth plane respectively.

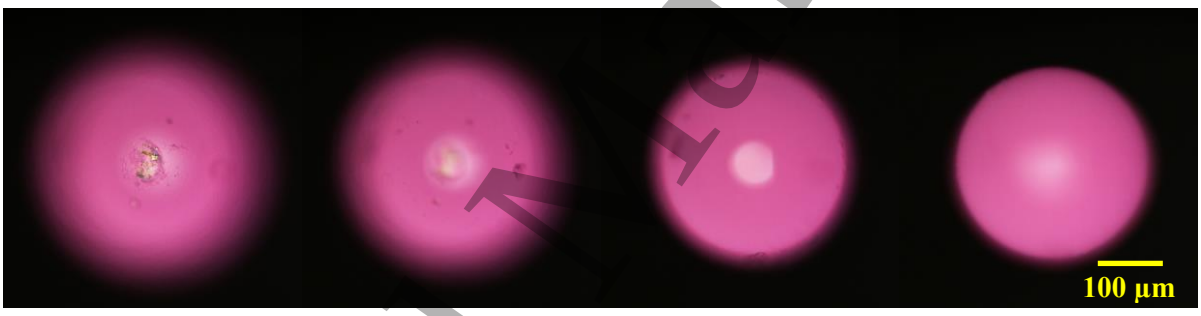

Figure 11. Microscope images of a 300 µm stylus tip at various height levels.

It is clear that different parts of contamination appear in focus in each of the images, while the majority of the sphere is blurred. Figure 12(a) shows the reconstructed FDoF image, with and without the use of polarising filters to eliminate the glare from the epi-illumination.

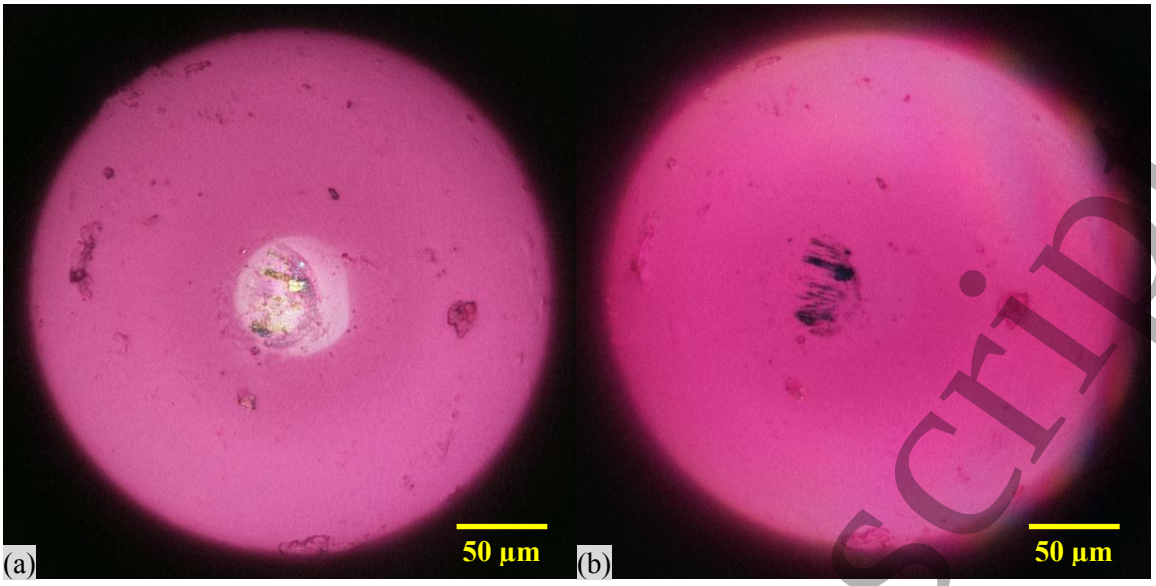

Figure 12. Reconstructed FDoF images of a 300 µm stylus tip using image stacks obtained (a) without polarising filters and (b) with polarising filters.

Reconstruction of the image stack has allowed all debris visible to the microscope to be presented in one image at the same time. Lateral optical resolution at 20× magnification (NA = 0.45) is about 0.7 µm. Debris as small as 1 µm (in pixel size) has been detected in Figure 12(a).

A bright light spot is observed at the centre of the sphere top in Figure 12(a), obscuring image contrast in the local area. This is likely due to the smooth ruby sphere acting as a micro lens. When focusing at about 90 µm from the top of the sphere, the light spot appears in contrast as shown on the third image in Figure 11. Corrections can be made to the image stack to lower the contrast of the light spot at certain height levels, but the procedure is tedious. Instead, by applying the polarising filters during the capture of the image stack, the light spot can be completely removed, as shown in Figure 12(b). The polarising filters significantly reduce the amount of light that is directly reflected from the tip surface onto the imaging sensor, but allows scattered light to pass through. Debris at the top of the sphere becomes clearly presented. However, metallic debris and scuff marks no longer appear shiny in the image. This is likely due to directly reflected light from these debris being filtered out by the polarising filters. For the same reason, the light spot is also filtered out. The image appears noisier and the azimuth plane does not appear as clear as in Figure 12(a).

As discussed in section 2.7, transparency of the ruby material can cause significant difficulties in stylus inspection. Figure 13 demonstrates such difficulty using FDoF images of two styli that were imaged from the side instead of from on top. The cause of this issue lies in the difference in the stylus assembly process. The 300 µm stylus tip is mounted onto a shaft using adhesive, while the 500 µm stylus tip is first drilled and then wrung into the shaft.

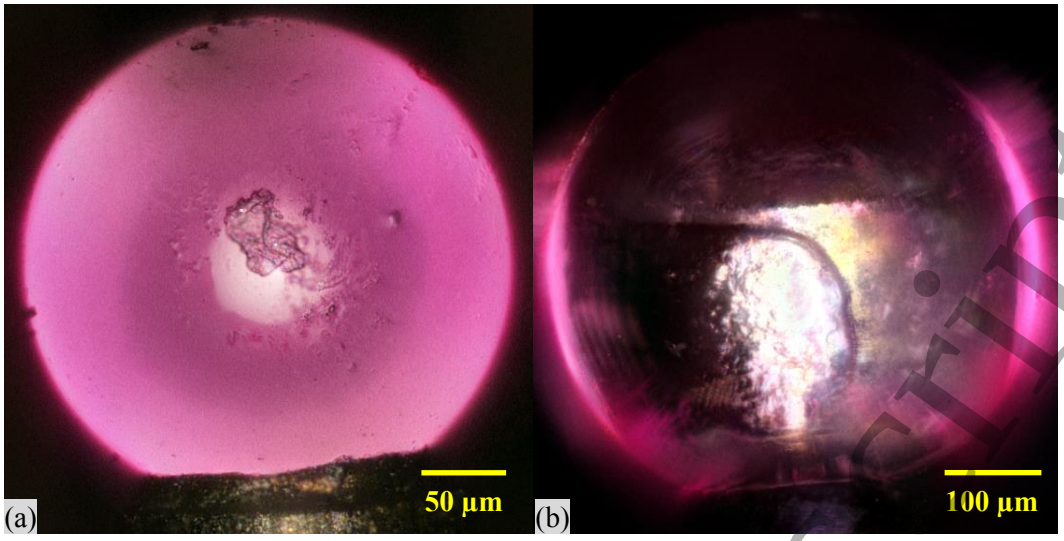

Figure 13. Reconstructed FDoF images of (a) a 300 µm stylus tip and (b) a 500 µm stylus tip.

Any contamination on the surface of the 500 µm stylus tip is obscured by the shaft inside the sphere. This is due to the shaft surface also appearing in focus when scanning through the sphere. Therefore, styli assembled using this process is not suitable for the proposed inspection technology. Fortunately, µCMM stylus tips are often smaller than 300 µm in diameter and mounted using adhesive instead of wringing. Tips smaller than 100 µm in diameter are usually made of metal using EDM/ECM processes followed by precision polishing. These metal tips are not transparent and therefore are also suitable for the proposed approach.

3.2 Stylus #2: 125 µm diameter

To further demonstrate the efficacy of the proposed approach, the smallest µCMM stylus commercially available with a ruby sphere is inspected. The stylus has a tip diameter of 125 µm and is used on the state-of-the-art µCMM Zeiss F25.

The stylus tip was imaged at 50× magnification (NA = 0.8) to take the advantage of higher resolving power while keeping the sphere in the FoV. DoF of the objective is approximately 1 µm, which would require at least 63 images to reconstruct a regular FDoF image. To reduce the number of images to be obtained for focus stacking, a total of 28 images were obtained instead. Step distance $\Delta z = 2$ µm was applied to the first 18 images and $\Delta z = 3$ µm to the last 10 images. A larger step distance was applied to high slope angle regions because the same vertical depth range corresponds to a smaller lateral area when projected onto the captured 2D image.

The reconstructed FDoF image of the stylus is shown in Figure 14.

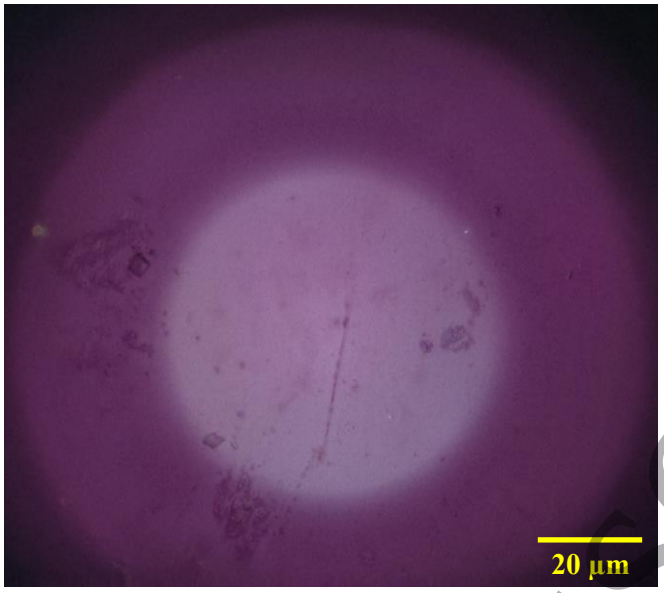

Figure 14. Reconstructed FDOF image of a 125 µm stylus tip using the proposed approach.

Sharpness of the image appears less than ideal due to the reduction in the number of images. Nonetheless, debris as small as 400 nm (optical resolution) in size can be detected in the image, demonstrating the efficacy of the proposed approach even when a reduced number of images are obtained. In the next section, the implementation of the proposed microscopy approach is discussed.

4. Prototype device for *in situ* stylus inspection

As the performance of the microscopy approach has been demonstrated, this section further demonstrates the effective implementation of this technology under the more relaxed constraints of a conventional CMM system. While demonstration of the proposed approach was previously conducted using a stand-alone microscope and obtaining of the stack of images was performed through manual adjustment of the height of the stylus, the implementation of this approach described in this section will further demonstrate the integration of the prototype inspection device with the CMM, where stylus inspection is performed *in situ* on a CMM and without human intervention; high precision movement of the stylus is performed automatically by the CMM; the capture of the stack of images is automated through communication with the CMM software. Furthermore, an example of automated stylus inspection at regular intervals (e.g. determined by the number of probing contacts made since last inspection) is provided to demonstrate the necessity of regular stylus inspection.

4.1 Setup

The implemented inspection system, as shown in Figure 15, consists of the following components:

(i) a microscope with reasonably small size,
(ii) a digital camera with an adapter to the microscope,
(iii) wired or wireless communication with the PC (not shown in the figure) running CMM measurement programs, and
(iv) software for image processing.

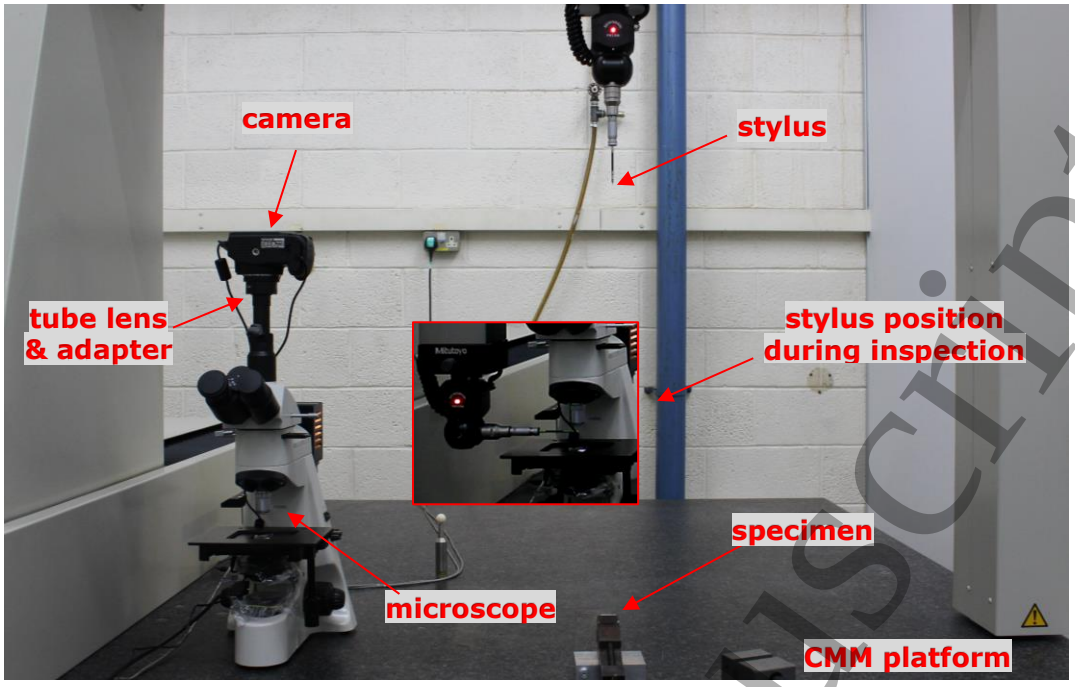

Figure 15. Setup of the focus stacking inspection system integrated with the CMM.

An upright microscope with epi-illumination setup is positioned on the platform of Mitutoyo Crysta-Apex C-121210 CMM. Measurement task is performed by probing the specimen placed in the workspace, which is paused at regular intervals to perform stylus inspection. The captured image stacks are automatically processed by Zerene Stacker and the amount of contamination is quantified using an image processing procedure.

The stylus mounted on the CMM probe has a ruby sphere of 300 µm diameter. Step movement of the stylus is achieved using the CMM's precision positioning capability, which improves the quality of the results. A consumer digital single-lens reflex camera Nikon D3200 is used to capture microscope images through a tube lens and an adapter. Stylus movement and image acquisition are synchronised through communication between the CMM software MCOSMOS and the image capture software.

4.2 Contamination quantification

For *in situ* stylus inspection, a quantified measure of the amount of contamination is often preferred by the user along with the image. In this study, Matlab is used to process the reconstructed FDoF images and estimate the area of the sphere surface being contaminated. The following image processing steps are followed:

(i) an edge detection algorithm is used to find the edge of the features,
(ii) a 2D median filter is used to reduce false contrast due to imaging noise,
(iii) the features are dilated to compensate for reduced feature size due to the median filter,
(iv) the closed edges are filled, and
(v) the remaining false edges due to glare and the sphere azimuth are corrected.

Figure 16 shows the FDoF images of a 300 µm stylus tip before and after being contaminated in three separate occasions after repeatedly probing on a nickel specimen.

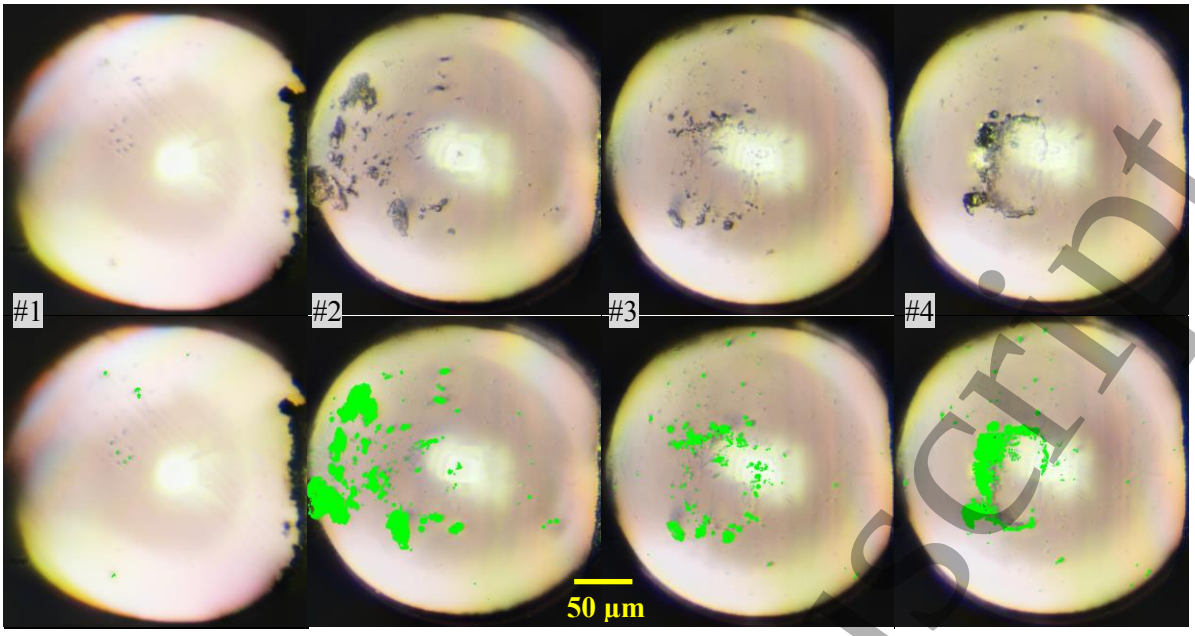

Figure 16. Reconstructed FDoF images of a 300 µm stylus tip (top) and contamination being identified using image processing in Matlab (bottom).

Although the microscope (with 40× plan objective and NA of 0.6) involved in the prototype setup is of lower quality than the Nikon LV100ND previously evaluated, sub-micrometre debris is still able to be detected in the images. The smallest debris is often neglected by the quantification procedure; but the majority of identified contamination agrees with visual inspection.

4.3 In situ stylus inspection

To demonstrate the efficacy of the proposed microscopy approach for *in situ* stylus inspection, a measurement program has been prepared and executed in the software MCOSMOS, where inspection of the stylus was conducted in-between measurements without human intervention. A stylus with 300 µm tip diameter was used to probe on a nickel specimen. Both the stylus and the specimen had been cleaned in an ultrasonic bath immediately before the measurement program was executed.

Inspection of the stylus was set to commence after every 50 contact points until 300 contacts have been made, after which inspection was set to commence after every 300 contacts. Progressive build-up of contamination on the stylus tip throughout the measurement program is visualised in Figure 17.

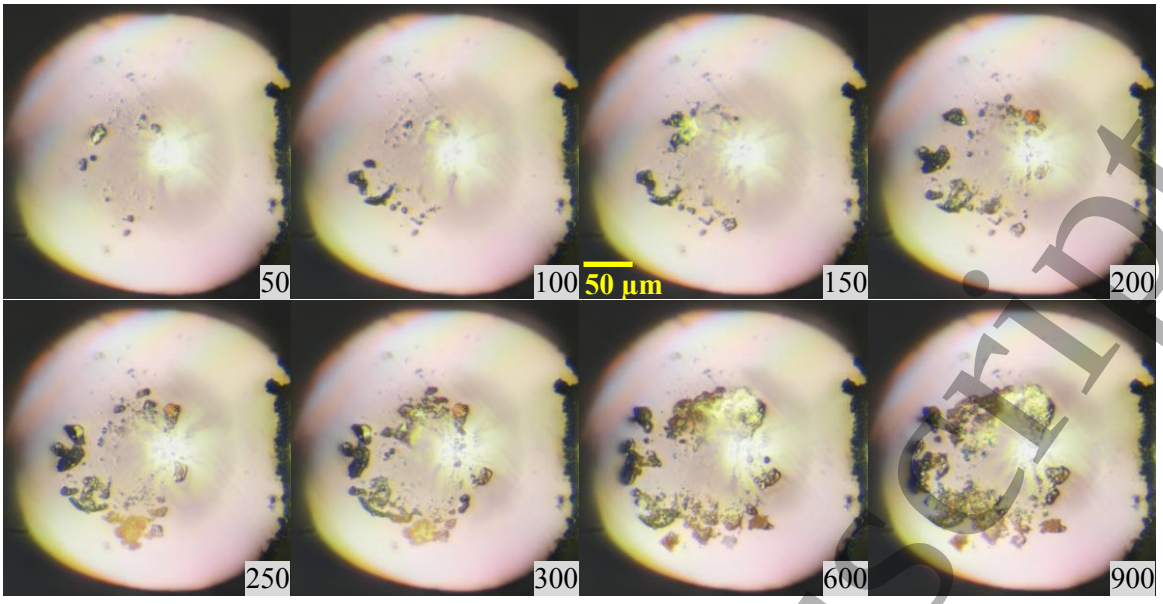

Figure 17. FDoF images of a 300 µm stylus tip obtained in line during measurement of 900 contacts in total using the proposed microscopy approach.

Using the quantification method described in section 4.2, the amount of contamination on the stylus tip is shown in Figure 18. The relevant amount of contamination is calculated as the area identified as contamination divided by the sphere surface area.

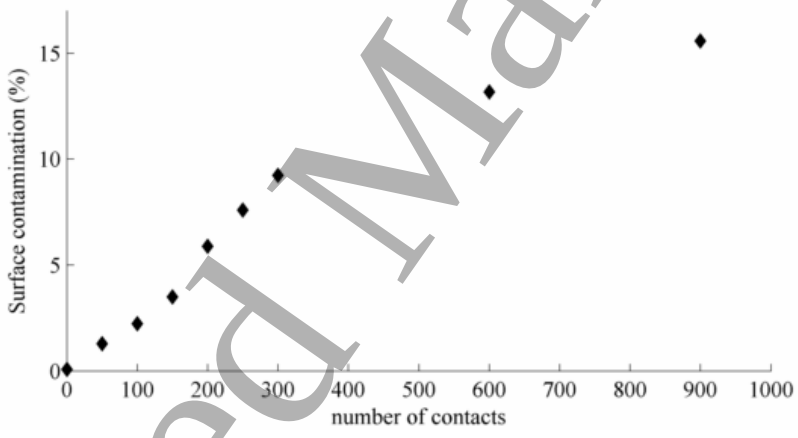

Figure 18. Amount of contamination on a 300 µm stylus tip during measurement of 900 contacts.

A steady increase of contamination on the stylus as measurement progressed has been observed. Although measurement error cannot be easily determined without knowing the material properties of the debris, it is reasonable to believe that measurement accuracy deteriorates as contamination builds up on the stylus tip. This prototype device was further used to perform inspection of stylus contamination over a data set of more than 20,000 contacts [14].

In an industrial environment, an empirically determined threshold value can be set and used to trigger an action once excessive contamination is detected. The following action may be to stop measurement and alert the operator for stylus cleaning. To achieve a fully automated procedure, a stylus cleaning method developed [11] by the authors can be used to execute another CMM subroutine to conduct stylus cleaning *in situ*. Re-inspection of the stylus is necessary after cleaning in order to verify cleanliness of the stylus tip.

4.4 Miniaturisation & multiple angle

An upright microscope was chosen to demonstrate the feasibility of the proposed approach in this study. For integration into a µCMM system, a compact microscope as illustrated in Figure 19 is preferred due

to the limited working volume of the CMM, and the microscope may pivot around the stylus for full inspection of the entire sphere.

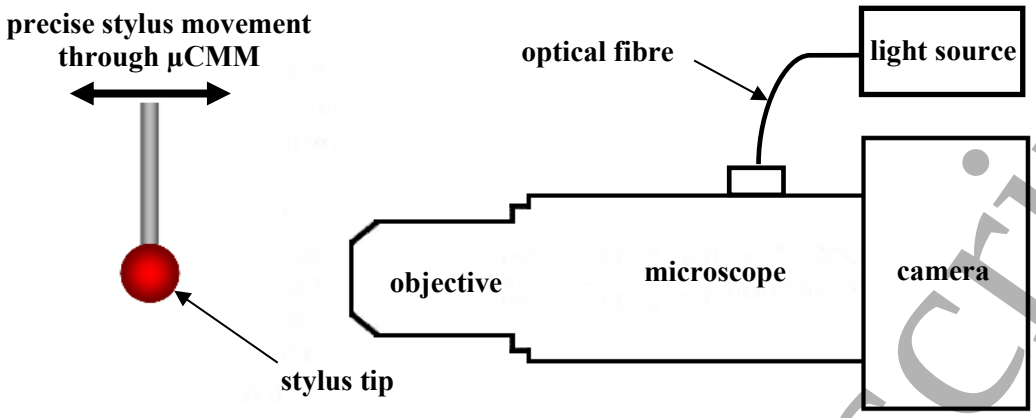

Figure 19. Illustration of a miniaturised stylus inspection system.

5. Conclusions

This study sets out to explore *in situ* inspection of µCMM stylus tips in order to monitor build-up of contamination on the stylus and prevent significant measurement error. The technical challenges for *in situ* stylus inspection have been identified and used to evaluate a series of commonly used non-contact surface inspection technologies. The capability and limitation of each technology were determined experimentally. Based on the findings of the evaluation, a microscopy approach has been proposed for inspecting the µCMM stylus tip for contamination. Through the use of a reflected light microscope and image processing methods, the proposed approach has proved effective in detecting debris as small as 400 nm. Subsequently, a prototype system using the proposed approach has been developed to perform *in situ* stylus inspection at regular intervals during a CMM measurement program. Quantified results have shown contamination to steadily build up on the stylus surface during measurement of a cleaned specimen. In an industrial environment, a threshold value may be set up to call for stylus cleaning once excessive contamination is detected to avoid unreliable measurements.

Implementation of the proposed approach, including recommended modification to the current prototype device, costs significantly less than other instruments evaluated in the study. More importantly, the approach is capable of inspecting the entire tip sphere and detecting contamination with sub-micrometre resolution in the matter of a few minutes.

The filtering applied during contamination quantification and the distortion caused by computing the contamination coverage on a sphere surface using 2D images will cause errors in the true contamination coverage. These two aspects will be investigated in future development.

Acknowledge

This study was funded by the European Metrology Research Programme (EMRP). The EMRP is jointly funded by the EMRP participating countries within EURAMET and the European Union. The authors would like to thank Prof. Richard Leach for his inputs on instrument costs, and Cyril Lacorne and Gustavo Queiroz Fernandes for their work in contamination quantification. The authors would also like to appreciate the support of Sensofar Merology and the Precision Manufacturing Centre at the University of Nottingham for assisting this project.

References

[1] Kinnell PK, Habeb RR. An evaluation of cleaning methods for micro-CMM probes. Meas Sci Technol. 2013; 24(8): 085603

[2] Chao ZX, Tan SL, Xu G. Evaluation on the probing error of a micro-coordinate measuring machine. in SPIE 7155. 2008.

[3] Gaoliang D, Sebastian B, Frank P, Hans-Ulrich D. A high precision micro/nano CMM using piezoresistive tactile probes. Meas Sci Technol. 2009; 20(8): 084001

[4] Anaïs N, Alain K, Felix M. Study of sapphire probe tip wear when scanning on different materials. Meas Sci Technol. 2012; 23(9): 094016

[5] Tsai CF, Cheng CC, Sheu DY. Investigating Micro Spherical Stylus Tips Fabrication by Electro Chemical and Single Pulse Electro Discharge Processes. Procedia CIRP. 2013; 6: 605-608

[6] Sheu D-Y. Manufacturing tactile spherical stylus tips by combination process of micro electro chemical and one-pulse electro discharge technology. Int J Adv Manuf Technol. 2014; 74(5-8): 741-747

[7] Küng A, Meli F, Thalmann R. Ultraprecision micro-CMM using a low force 3D touch probe. Meas Sci Technol. 2007; 18(2): 319

[8] Flack D, Claverley J, Leach R. Chapter 9 - Coordinate Metrology. In: R Leachs, editor. Fundamental Principles of Engineering Nanometrology (2nd Edition), Oxford: William Andrew Publishing; 2014

[9] International Organisation for Standardization. *ISO 10360-5:2010 Geometrical product specifications (GPS) - Acceptance and reverification tests for coordinate measuring machines (CMM) - Part 5: CMMs using single and multiple stylus contacting probing systems*. 2010: Geneva, CH

[10] Feng X, Lawes S, Kinnell P. *Evaluation of the Capabilities and Damage Risk of Cleaning Methods for Micro-CMM Stylus Tips*, in *Proceedings of the 4M/ICOMM2015 Conference*. 2015: Milan, Italy

[11] Feng X, Kinnell PK, Lawes S. Development of CO2 snow cleaning for in situ cleaning of µCMM stylus tips. Meas Sci Technol. 2017; 28(1): 015007

[12] Brecko J, Mathys A, Dekoninck W, Leponce M, VandenSpiegel D, Semal P. Focus stacking: Comparing commercial top-end set-ups with a semi-automatic low budget approach. A possible solution for mass digitization of type specimens. ZooKeys. 2014; (464): 1-23

[13] Adelson EH, Anderson CH, Bergen JR, Burt PJ, Ogden JM. Pyramid methods in image processing. RCA engineer. 1984; 29(6): 33-41

[14] Feng X, Kinnell P, Lawes S. Contamination of µCMM stylus tips on-machine inspection. in euspen 16th International Conference. 2016. Nottingham, UK